

10. GEOTHERMAL REGIME OF THE WESTERN MARGIN OF THE GREAT BAHAMA BANK¹

Seiichi Nagihara² and Kelin Wang³

ABSTRACT

The geothermal regime of the western margin of the Great Bahama Bank was examined using the bottom hole temperature and thermal conductivity measurements obtained during and after Ocean Drilling Program (ODP) Leg 166. This study focuses on the data from the drilling transect of Sites 1003 through 1007. These data reveal two important observational characteristics. First, temperature vs. cumulative thermal resistance profiles from all the drill sites show significant curvature in the depth range of 40 to 100 mbsf. They tend to be of concave-upward shape. Second, the conductive background heat-flow values for these five drill sites, determined from deep, linear parts of the geothermal profiles, show a systematic variation along the drilling transect. Heat flow is 43–45 mW/m² on the seafloor away from the bank and decreases upslope to ~35 mW/m². We examine three mechanisms as potential causes for the curved geothermal profiles. They are: (1) a recent increase in sedimentation rate, (2) influx of seawater into shallow sediments, and (3) temporal fluctuation of the bottom water temperature (BWT). Our analysis shows that the first mechanism is negligible. The second mechanism may explain the data from Sites 1004 and 1005. The temperature profile of Site 1006 is most easily explained by the third mechanism. We reconstruct the history of BWT at this site by solving the inverse heat conduction problem. The inversion result indicates gradual warming throughout this century by ~1°C and is agreeable to other hydrographic and climatic data from the western subtropic Atlantic. However, data from Sites 1003 and 1007 do not seem to show such trends. Therefore, none of the three mechanisms tested here explain the observations from all the drill sites. As for the lateral variation of the background heat flow along the drill transect, we believe that much of it is caused by the thermal effect of the topographic variation. We model this effect by obtaining a two-dimensional analytical solution. The model suggests that the background heat flow of this area is ~43 mW/m², a value similar to the background heat flow determined for the Gulf of Mexico in the opposite side of the Florida carbonate platform.

INTRODUCTION

Before Ocean Drilling Program (ODP) Leg 166, there were very few direct geothermal measurements in offshore Florida-Bahama carbonate platforms. There has been no report of measurements using conventional marine heat-flow probes such as those described by Bullard (1954), Jemsek et al. (1985), and Lister et al. (1990). This is probably because of the difficulty associated with determining geothermal heat flow in a shallow-water environment. Much of the seafloor in the Straits of Florida is shallower than 800 meters below sea level (mbsl). There is significant seasonal fluctuation in the temperature of the bottom seawater (e.g., Niiler and Richardson, 1973). Normally, a geothermal probe penetrates only 5–7 meters below seafloor (mbsf), while the thermal noise associated with the seasonal fluctuation may penetrate deeper than 10 mbsf. Some borehole temperature measurements were reported offshore of southwestern Florida (Buller et al., 1984), but the Bahama platform was virtually “untouched.” The in situ bottom-hole temperature data from Leg 166, which were obtained in depths of 30–300 mbsf, may provide the first direct information on the thermal regime of the platform.

IN-SITU BOTTOM-HOLE TEMPERATURES AND THERMAL CONDUCTIVITIES OBTAINED DURING LEG 166

A total of 62 reliable in situ bottom-hole temperature measurements were made at Sites 1003 through 1009 (Fig. 1). Two types of instrumentation were used for the measurements: the Adara temper-

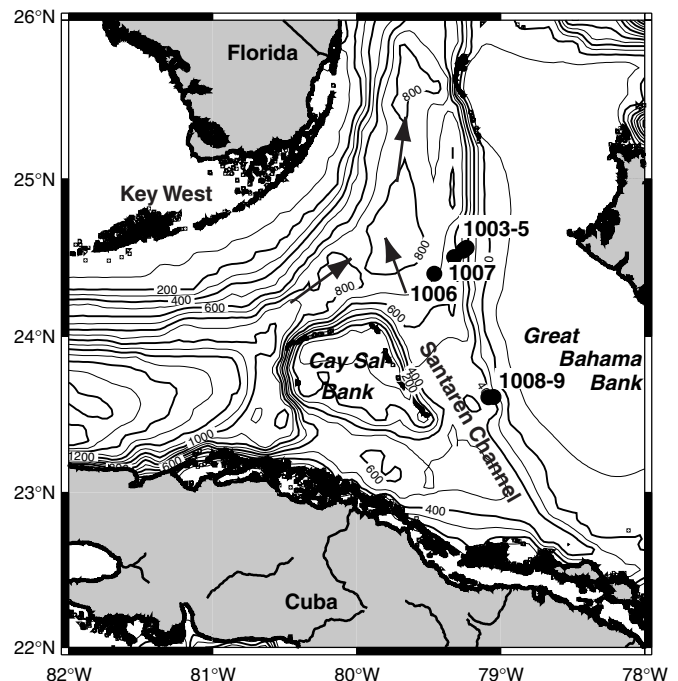


Figure 1. Bathymetric map of the Straits of Florida. The locations of the drill sites (numbered) are indicated by solid circles. Also shown are flow directions of the currents.

ature tool, which was built into the cutting shoe of the advanced piston corer (APC), and the water-sampling temperature probe (WSTP) with its water sampler turned off. These instrumentations have been described in Eberli, Swart, Malone, et al. (1997) and previous ODP publications such as Fisher and Becker (1993). The Adara tool records the temperature while the APC is held at the bottom of the

¹Swart, P.K., Eberli, G.P., Malone, M.J., and Sarg, J.F. (Eds.), 2000. *Proc. ODP, Sci. Results*, 166: College Station TX (Ocean Drilling Program).

²Department of Geosciences, University of Houston, 4800 Calhoun, Houston TX 77204-5503, USA. nagihara@uh.edu

³Pacific Geoscience Centre, Geological Survey of Canada, 9860 West Saanich Road, Sidney, B.C. V8L 4B2, Canada.

hole for ~10 min. The WSTP temperature sensor is mechanically inserted into the bottom-hole sediments separately from coring. Both tools record the temperature of the bottom-hole sediments as they cool down from a higher temperature associated with the frictional heat of the probe insertion. The equilibrium temperature of the sediment is determined by theoretical extrapolation of this cooling curve. The cooling of the Adara sensor is modeled as the conductive heat loss through the surface of a metal cylinder (Horai and Von Herzen, 1985), and the cooling behavior of the WSTP sensor is approximated by the conductive heat loss of a solid rod (e.g., Bullard, 1954). These simple one-dimensional theoretical models are not necessarily applicable to a very early portion of the cooling curve, which is more influenced by the thermal properties of the metal casing. Also, the late portion of the cooling curve is influenced by vertical heat conduction along the probe. Thus, we carefully chose a middle part of each temperature record for reliable estimation of the equilibrium temperature. For each temperature record, we made 5–10 temperature determinations by choosing slightly different time windows. The variation among these temperature values is the basis for error estimation.

A total of 666 thermal conductivity measurements were made on board on unconsolidated core samples from Sites 1003 to 1009. The standard needle-probe technique (Von Herzen and Maxwell, 1959) was used for these measurements. The temperature and conductivity values and their quality analyses have been reported in Eberli, Swart, Malone, et al. (1997).

THERMAL CONDUCTIVITIES OF LITHIFIED CORE SAMPLES

The thermal conductivity measurements made during Leg 166 were limited to relatively shallow, unconsolidated sediments. To better constrain the thermal properties of deeper sediments, we measured thermal conductivities of 14 lithified samples from Holes 1003C, 1005C, and 1007C using the divided-bar method after the cruise (Table 1). The technique of the divided-bar conductivity measurement has been described previously by a number of authors (e.g., Birch, 1950; Carslaw and Jaeger, 1959, p. 139; Turcotte and Schubert, 1982, p. 135; Lewis, 1975). We used the apparatus at the Pacific Geoscience Centre, Geological Survey of Canada, Sidney, British Columbia. Each sample was prepared to be in cylindrical shape of 24.9–25.4 mm in diameter and 14–32 mm in thickness. The planar top and bottom surfaces of the samples were made as smooth as possible to achieve good thermal contact with the divided bar. The samples were soaked in water for ~24 hr before the measurements. The apparatus was calibrated using fused quartz discs of the same diameters but different thicknesses. The conductivity measurements were repeatable within 5%.

OBSERVATIONS

We focus mainly on the geothermal data obtained at five drill sites (Sites 1003 through 1007) located along an east-west transect of the western margin of the Great Bahama Bank (Fig. 1). Figure 2 shows plots of temperature vs. depth and thermal conductivity vs. depth for these five sites. It also shows plots of the temperature against the cumulative thermal resistance (Bullard plots after Bullard, 1939) for the same sites. The thermal resistance of a depth interval is defined by the thickness of the interval divided by the thermal conductivity.

The geothermal profiles at these five drill sites show significant curvature in the upper 50–100 mbsf (Fig. 2). At Site 1003, the profile is slightly concave-upward in the upper 35–70 mbsf and is concave-downward in the depths below. At Site 1004, the uppermost two temperature points deviate positively from the linear trend of the lower points and the profile is concave upward. At Site 1005, the uppermost two points deviate negatively and the geothermal profile in the upper 60 mbsf is concave upward. Site 1006 exhibits a concave-upward

Table 1. Thermal conductivities of lithified core samples from the Leg 166 holes.

Core, section, interval (cm)	Depth (mbsf)	Conductivity (W/[m-K])
166-1003C-		
2R-1, 65-69	416.2	2.02
19R-, 73-75	627.4	1.91
22R-1, 42-45	656.1	1.77
35R-5, 140-143	786.6	1.97
47R-1, 13-15	896.1	2.21
69R-1, 91-93	1108.7	1.87
88R-4, 80-82	1295.7	1.79
166-1005C-		
3R-1, 131-134	406.5	2.17
14R-2, 73-77	509.0	2.12
24R-1, 87-91	599.9	2.45
166-1007C-		
30R-3, 44-45	584.3	2.17
41R-3, 130-134	690.6	2.14
63R-3, 56-60	901.8	2.34
91R-5, 41-44	1174.3	2.15

profile most clearly from 30–100 mbsf. Closely spaced temperature measurements are available from this site from the Adara/APC deployments. Some temperature determinations at shallow depths have relatively large uncertainties (~1°C) because the corer sometimes moved during measurement in sediments that were relatively soft. At Site 1007, the uppermost two points deviate negatively from the linear trend. All the sites show some degree of concave-upward curvature except for Site 1007.

The curvature is also seen in the Bullard plots (Fig. 2), which should make a straight line for a steady state thermal regime. For all the sites, it is not possible to draw a straight line within the uncertainties of the individual temperature measurements. Site 1006, which yields the most detailed profile of the bottom-hole temperature, demonstrated the curvature most clearly. The curvature of the Bullard plots suggests that the perturbation of the temperature profile cannot be accounted for by the downhole variation in thermal conductivity. Either the thermal regime is not in steady state or there is a significant, convective component in the total heat budget at these relatively shallow depth ranges. More specifically, three mechanisms can be responsible for a concave-upward geothermal profile. The first is a recent increase in sedimentation rate. The second is recent increase in bottom water temperature (BWT). The third is influx of seawater into the sediments. We discuss these possibilities in the next section.

At all sites except Site 1003, the points below 70–100 mbsf in the Bullard plots show a linear trend clearly. The conductive heat flow can be determined from these deep portions of the measurements. We obtain the heat flow as the slope of the Bullard plot (Fig. 2). We calculate the standard error for each heat-flow determination using Student *t*-distribution with 90% confidence level. In Figure 2, the data points used in the heat-flow determination are shown as closed circles and those omitted are shown as plus signs. The heat-flow values at these sites show a very systematic variation along the transect (Table 2). From the west to east, heat flow decreases upslope. The lateral variation in heat flow is discussed in the next section.

DISCUSSION

We first discuss the potential causes of the curvature of the geothermal profile and then the lateral variation in heat flow along the transect.

Thermal Effect of Sedimentation

If sedimentation occurs very rapidly with little interruption, it prevents the shallow sedimentary formation from achieving a steady thermal state. As a result, the conductive heat flow measured at a shallow sub-bottom depth can be significantly less than the actual

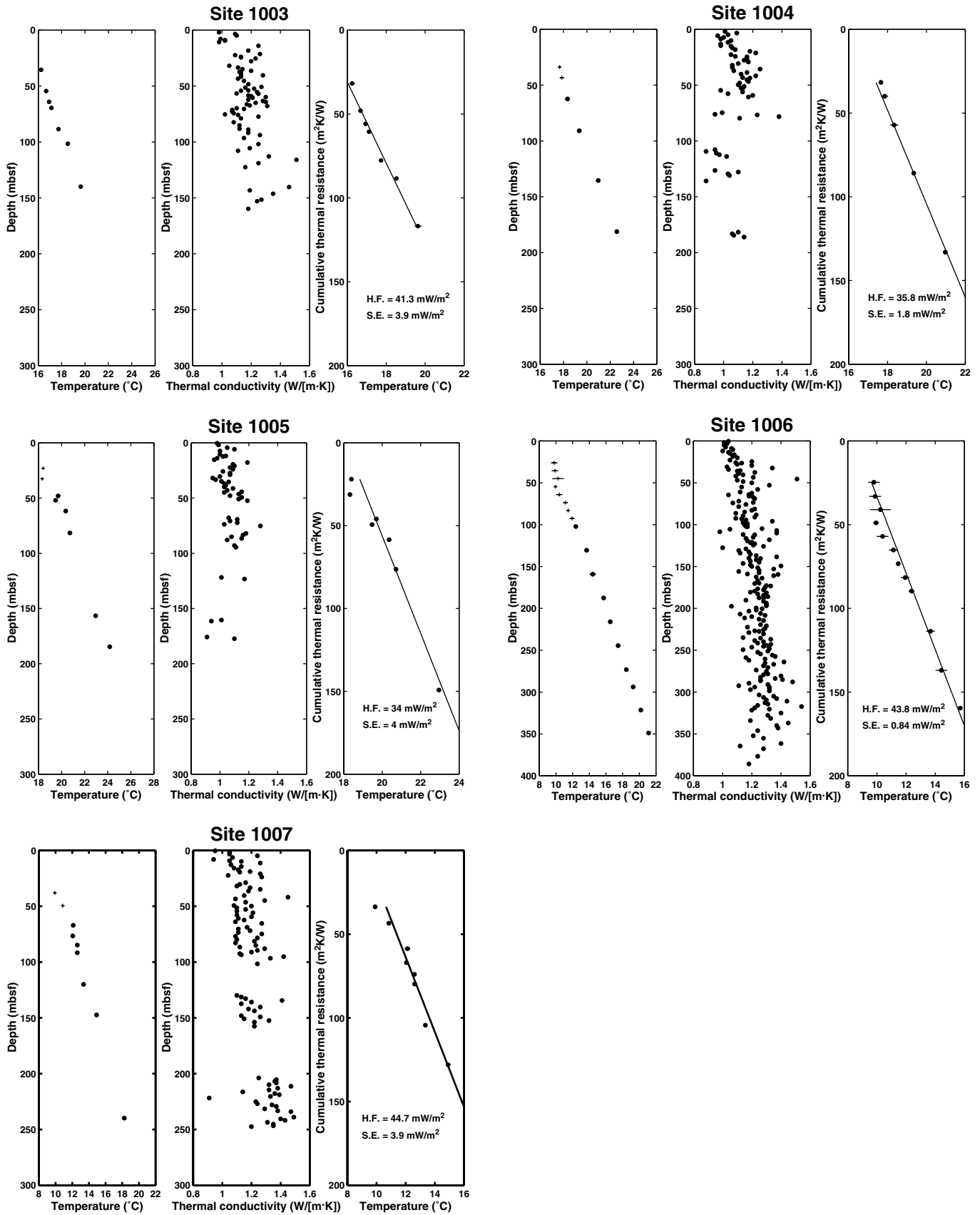


Figure 2. Temperature vs. depth, thermal conductivity vs. depth, and temperature vs. cumulative thermal resistance plots for Sites 1003 through 1007. In the first plot for each site, + = data points not included in the heat-flow determination.

Table 2. Heat flow values determined for the Bahama Transect sites.

Site	Conductive heat flow (mW/m ²)	Standard error (mW/m ²)	Sedimentation effect (% of total heat flow)
1003	41.3	3.9	-3
1004	35.8	1.8	-2
1005	34.0	4.0	-2
1006	43.8	0.8	-2
1007	44.7	3.9	-2

geothermal heat flow entering from the bottom of the formation. The thermal effect of sedimentation can be evaluated through mathematical modeling if (1) the sediment accumulation history, (2) the thermal properties of the sediments, and (3) the history of heat input from the basement at the site have already been well constrained. The mathematical models proposed earlier solved the one-dimensional heat conduction equation for a semi-infinite solid with a moving surface boundary. (e.g., Von Herzen and Uyeda, 1963; Jaeger, 1965). More recent models account for the effects of the sediment compaction and the resultant vertical pore-fluid expulsion (e.g., Hutchison 1985). This study uses the latter approach in evaluating the thermal effect of sedimentation.

In the mathematical model, the sediment accumulation history must be constructed from the very beginning of the basin (Jurassic or Triassic?; Eberli, Swart, Malone et al., 1997). At Sites 1003 through 1007, recent sedimentation rates can be determined from the biostratigraphic data from the drill sites (Eberli, Swart, Malone, et al., 1997). Particularly, Sites 1003 and 1007 provide data from early Miocene to Holocene. We calculate the average sedimentation rate for each depth interval dated by microfossils. In doing so, we account for the effects of sediment compaction (e.g., Sclater and Christie, 1980). For older sediments that could not be reached by the drilling, we use the information available from the seismic reflection profiles along the drill sites (Eberli et al., 1994; Eberli, Swart, Malone, et al., 1997). The seismic data do not show the basement, but they penetrate to Mid-Cretaceous sequences that are ~1.5 km sub-bottom depth. We estimate the thickness of the earlier Mesozoic sequences to be ~1 km based on the seismic data from the neighboring Florida platform (Schlager et al., 1984). Thus, we use a total sediment thickness of 2.5 km in the model. We assume that the oldest sediment was deposited at 150 Ma. Knowing the thickness and the bottom age of the sedimentary layer, we obtain the average sedimentation rate for the old sediments and use it in the model. The simplification of accumulation history of old sediments affects the model result very little because it is the recent sedimentation history that controls the shallow thermal regime.

In modeling the compaction of sediments and their physical properties, we use the conventional, exponential compaction curve:

$$\phi = \phi_0 \exp\left(-\frac{z}{\lambda}\right),$$

where ϕ is the porosity, z is the sub-bottom depth, ϕ_0 is the porosity at seafloor, and λ is a constant determined empirically. The thermal conductivity of the sediment varies with porosity. We use the formula by Budiansky (1970) to calculate the bulk sediment conductivity:

$$K = \frac{-\alpha + \sqrt{\alpha^2 + 8k_s k_w}}{4},$$

where $\alpha = 3\phi(k_s - k_w) + k_w - 2k_s$, with k_s and k_w being the sediment and water thermal conductivities, respectively. By fitting the two equations to the physical properties measurements made during Leg 166 (Eberli, Swart, Malone, et al., 1997) and the thermal conductivity measurements made in this study (Table 1), we determine ϕ_0 and λ for each site. Then, we calculate sedimentation rates using the

depths corrected for compaction. The real compaction curves are much more complex, but we believe that the long-term trend is fairly well represented by our model.

Little information is available on the time variation of heat input from the basement. However, the choice of the basement heat-flow parameters does not have as large an impact on the model results as the other parameters (Hutchison, 1985). Rather than introducing too many unconstrained parameters, we simply assume that the basement heat input varied in time just like that of a typical oceanic lithosphere cooling (Parsons and Sclater, 1977) for the past 150 m.y. This results in basement heat-flow values that are similar to what we have observed (35–40 mW/m²).

Our model also accounts for radiogenic heat production within the sediments. We use a heat production rate of 0.66 $\mu\text{W}/\text{m}^3$ for the solid component of the sediment, which was obtained from measurements made on lithified limestone samples from the Deep Sea Drilling Project Sites 535 and 540 off the Florida platform (Nagihara et al., 1996). The value is typical for limestones in general. In the model, the bulk heat production rate also varies with porosity.

The assumptions and the parameters defined above are incorporated into a finite-element model (Wang and Davis, 1992) and yield the thermal effect of sedimentation. This computation method is essentially the same as the algorithm of Hutchison (1985). Table 2 shows the model-predicted reduction in total heat flow because of the sedimentation effect. Probably, the estimates for Sites 1004, 1005, 1006 are less reliable than others because drill holes at these sites did not reach as deep. The model results show that reduction in heat flow is only 2%–3% for all sites. The effect is small, because the sedimentation rate rarely exceeded 100 m/m.y. for all the sites and for the entire period. Such rates are an order of magnitude smaller than those of typical clastic sedimentary basins. A few percent reduction in heat flow does not cause significant curvature in the geothermal profile, as shown in Figure 3 where we compare the actual geothermal profile with that predicted by the sedimentation model for Site 1004. Therefore, sedimentation is not the primary cause for the curvature in our temperature profiles in the shallow zones of sediments.

Influx of Seawater

In a relatively porous carbonate platform such as the Great Bahama Bank, pore-water movement is possible. The pore-water chemistry data from Sites 1003 through 1007 core samples seem to indicate that seawater flows into the top layers of the sediments because a number of elements, particularly chloride, show uniform concentration values in the upper 20–50 mbsf (Eberli, Swart, Malone, et al., 1997). If there is influx of cold water into the formation, it can cause a concave upward geothermal profile (e.g., Bredehoeft and Papadopoulos, 1965). Thus, it may explain some of our observations. For example, at Sites 1004 and 1005, this chemically inferred “flushed zone” is nearly 50 m thick. Site 1004 shows a concave-upward profile at depths shallower than 60 mbsf, though there are only three reliable measurements. At Site 1006, five temperature data points in the upper 60 mbsf also show a slight concave-upward feature.

At other sites, the correlation is not as good. There, the zone of nonlinear thermal profile extends much deeper than the chemically inferred flushed zone. At Site 1003, the flushed zone is ~50 m thick, whereas the slight concave feature in the temperature profile seems to reach 100 mbsf. At Site 1006, the chemically flushed zone is only 20 m thick, while the temperature profile shows a clear, concave-upward feature down to 100 mbsf. At Site 1007, the chemical flushed zone is ~20 m thick, while the temperature profile is concave downward in the top 50 mbsf and concave upward to ~120 mbsf.

The chemical diffusion coefficient of pore water is several orders of magnitude less than the thermal diffusivity. In other words, the chemistry data should be more sensitive to fluid movement than the thermal data. Vertical fluid movement could not perturb the geothermal profile without affecting the pore chemistry gradient, while the

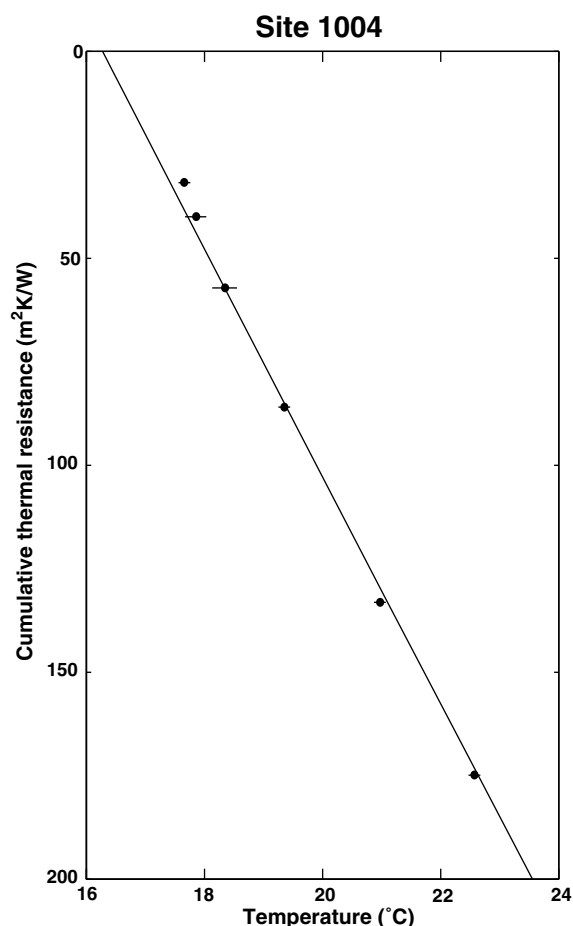


Figure 3. Comparison of the Bullard (temperature vs. cumulative thermal resistance) plot predicted by the model that accounts for the thermal effect of sedimentation (solid line) and the actual data (solid circles) at Site 1004.

opposite may be possible. Thus, if there is influx of water from the seafloor, the chemical anomaly should extend deeper than the thermal anomaly. At Sites 1004 and 1005, the thickness of the flushed zone is about the same as that of the anomalous geothermal profile. It is possible that the thermal regime of these two sites is affected by fluid movement. At Sites 1006 and 1007, the zone of thermal anomaly is thicker than the chemically inferred flushed zone, opposite from the theoretical expectation. In Figure 4, we describe in detail the nature of the shallow thermal anomaly at Site 1006. In this plot, we show the temperature deviation from the linear trend observed at greater depths (>100 mbsf; see also Fig. 2). The temperature variation is systematic in the upper 100 mbsf. The amplitude of temperature deviation increases steadily with depth in the top 60 mbsf and then decreases gradually to zero at near 100 mbsf (Fig. 4). In contrast, the profile of the chloride concentration shows a typical diffusive characteristic in the same depth range, increasing with a near-constant rate. Therefore, the curvature of the geothermal profiles at Sites 1006 and 1007 cannot be explained by influx of seawater. The same can be said for Site 1003, though the thermal anomaly is significantly smaller than that of Sites 1006 and 1007.

Temporal Fluctuation of Bottom-Water Temperature

We shall discuss now the third mechanism, long-term fluctuation of BWT, as a possible explanation for the curvature in the geothermal profiles. Even though a number of hydrographic measurements have been reported from this area (NOAA, 1994), no direct, long-term

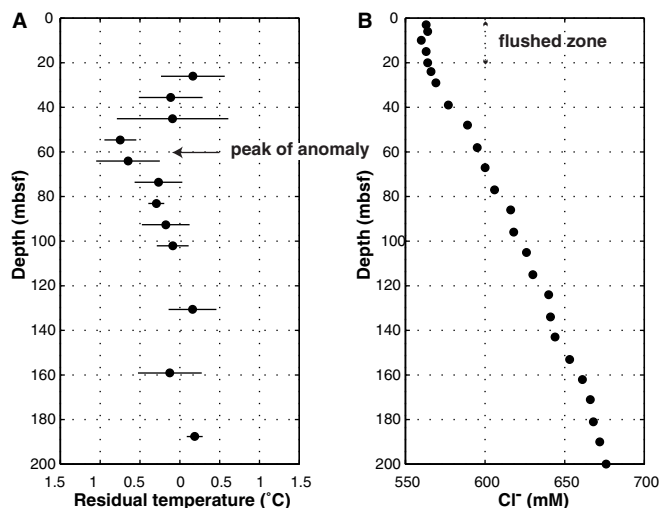


Figure 4. Comparison of the temperature deviation from (A) the linear trend and (B) the chloride concentration profile for Site 1006.

record of bottom-water temperature is available. However, more than 1°C of seasonal fluctuation has been reported at as deep as 600 mbsl (Niiler and Richardson, 1973). This depth is comparable to the seafloor depths of Site 1006 (669 mbsl) and Site 1007 (662 mbsl).

There may be significant interannual or interdecadal variation as well, but such a long-term trend is difficult to infer from the existing data because the hydrographic regime in the Straits of Florida is fairly complex (e.g., Leaman et al., 1995). The Site 1006–1007 area is where the Florida current, which loops around western Cuba, meets other tributary flows through the channels of Northwest Providence, Santaren, and Old Bahama. Together they form the Gulf Stream (Fig. 1). Water entering from the Santaren Channel is considerably warmer and more saline than the main Florida current. There is a large, horizontal thermal gradient in the east-west direction in the area of the drill sites. Even at 400-m water depth, there is a temperature difference of more than 8°C over the 80-km distance between the Florida peninsula and the Great Bahama Bank. Superimposed over this general trend is the large seasonal variation in the currents. Therefore, unless a series of hydrographic measurements are made at fixed locations very frequently for a decade or two, it would be impossible to recognize any long-term variation of the water temperature distribution in the Straits of Florida.

There is, however, strong evidence that the intermediate to deep water of the Gulf Stream, which originates from the Straits of Florida, has warmed up considerably in the last three decades (Roemmich and Wunsch, 1984; Levitus, 1989; Parrilla, et al., 1994; Levitus and Antonov, 1995). The warming is 0.2°–0.5°C at 400 mbsl. In addition, ground-surface temperature of the same region has shown significant, decadal-scale variation in annual mean temperature. For example, weather stations in Key West (location in Fig. 1) show a clear cooling trend in late 19th century and a steady warming trend throughout the 20th century (Fig. 5) (see Hanson and Maul, 1993). It is possible that such long-term climatic changes affect the BWT of the Straits because even short-term, seasonal fluctuations affect it.

Site 1006 offers the most detailed temperature profile and exhibits the concave-upward curvature most clearly. Assuming that this curvature is caused by a temporal variation in BWT, here we attempt to reconstruct the history by mathematical models and examine whether or not it could be conformable with other hydrographic and climatic observations. If BWT changes over time, the thermal signal slowly propagates to the subsea formation and is overprinted to the regional background geothermal gradient. Thus, if a detailed geothermal profile can be obtained from a borehole, the history of the BWT can be reconstructed theoretically by solving the inverse heat conduction

problem (Wang, 1992). Inversion of borehole temperature data has been used on land and helped reconstruct the history of ground surface temperature for the past 100–200 years at over three hundred locations (e.g., Lachenbruch and Marshall, 1986; Pollack and Chapman, 1993; Deming, 1995).

We use a spectral inverse method based on the theory of one-dimensional heat conduction to reconstruct the BWT history at Site 1006. The inversion method was described by Wang (1992) and has been successfully applied to temperature data from land boreholes (Wang and Lewis, 1992; Wang et al., 1992; Kohl, 1998). Other methods for the same purpose are available (Shen and Beck, 1991; Beltrami and Mareschal, 1991), which yield similar results but differ in flexibility in incorporating a priori information as model constraints. Some detailed studies on data noise and model resolution can be found in Shen et al. (1995). In our calculation, the sub-bottom sediments are divided into seven layers, each having uniform thermal properties (Fig. 6). The diffusivities are estimated from the thermal conductivities assuming a volumetric specific heat capacity of $3.2 \times 10^6 \text{ J/m}^3\text{K}$.

The inverse problem is ill posed, and a priori constraints are required for a stable and unique solution. Basic constraints on the unknown BWT are its smoothness and boundedness. We introduced these constraints probabilistically by regarding the a priori BWT time series as a stationary Gaussian process with a Hamming autocovariance function. The a priori standard deviation and autocorrelation scale of the BWT are assumed to be, respectively, 1°C and 50 years. We did not include mudline temperature data into our calculation because they may have been affected by drillwater circulation.

The estimated BWT history is shown in Figure 7 and the fit to the borehole temperature is shown in Figure 6 (solid line). In the early 18th century, the long-term average BWT ($\sim 8.2^\circ\text{C}$) was $\sim 1^\circ\text{C}$ lower than the present value. It slowly cooled down to a minimum at year ~ 1900 , and then increased rapidly to the present temperature ($\sim 9.2^\circ\text{C}$). Readers should be reminded that the estimated BWT history is a smoothed one. It gradually loses temporal resolution as it looks further back in time. There might be large-magnitude, decade-scale variations prior to 100 or 200 years ago and the cooling could well be some rapid event(s), but the details cannot be resolved by geothermal data. The most reliable information in this reconstruction is (1) the long-term average in the past, (2) some cooling events up to year ~ 1900 , and (3) the recent fast warming trend. One can in fact correlate each of these features directly to the curvature of the measured temperature profile. For example, the upward decrease in temperature relative to the steady-state reference profile results from the cooling trend, and the increase further up results from the recent warming.

We should refrain from making a direct inference about climate change and global warming from the geothermally determined BWT because of the complexity of the ocean-climate interaction. However, we cannot help but notice the resemblance of the BWT history to the surface air temperature (SAT) history recorded in nearby Key West weather stations, which shows a clear cooling event in late 19th century and a steady warming trend throughout the 20th century (Fig. 5; Hanson and Maul, 1993). Ground surface temperature (GST) histories determined from land boreholes in eastern Canada by Wang et al. (1992) and Wang and Lewis (1992) also show very similar variations (Note: Because of a plotting error, the GST histories illustrated in these two references should have been shifted backward in time by 30 years). They all suggest that the recent warming started around the turn of the century, though they differ in magnitude, $\sim 1^\circ\text{C}$ at Key West and Site 1006, and $\sim 2^\circ\text{C}$ in southeastern Canada.

Presently there is not enough information to determine whether or not the correlation between the BWT history of Site 1006 and the data from Key West and eastern Canada is purely fortuitous. It is also difficult to apply a similar BWT history to the geothermal data from other drill sites. We did not attempt to reconstruct their BWT histories, but it seems obvious because the curvature of Site 1007 is significantly different from that of Figure 7. Although there are many pieces of circumstantial evidence that support the BWT fluctuation as

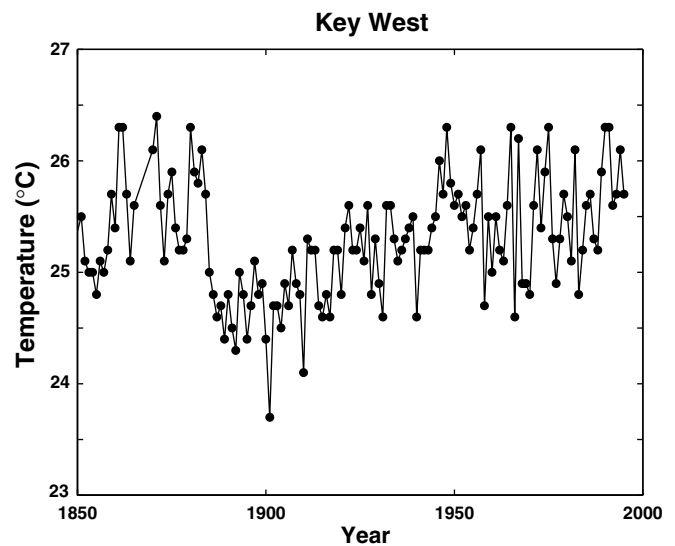


Figure 5. Surface air temperature records at weather stations in Key West for the past 150 yr.

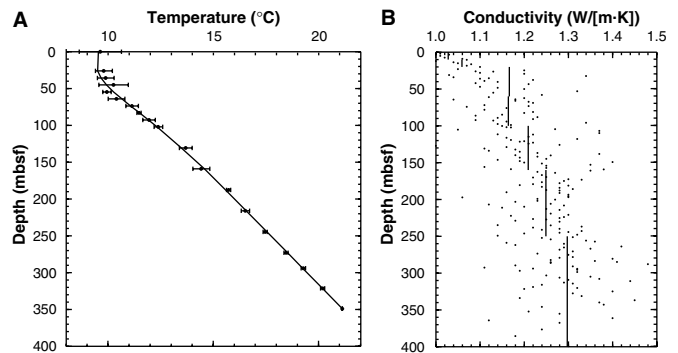


Figure 6. **A.** The bottom-hole temperatures measured at Site 1006 are compared with the geothermal profile for the BWT history given in Figure 7. **B.** The seven layers of different thermal conductivities are shown as vertical bars and compared with the actual measurements made on the cores recovered from Site 1006.

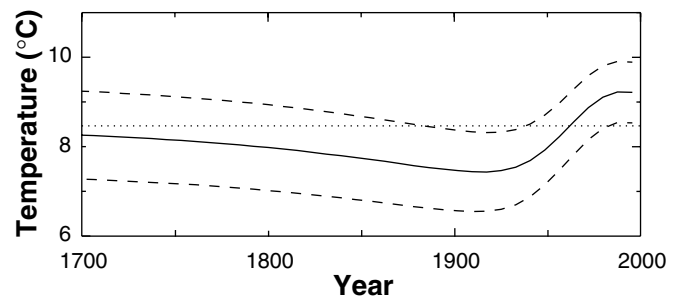


Figure 7. BWT history obtained by inverting the geothermal measurements at Site 1006. Dashed lines show one-standard-deviation error bounds. The dotted line is the estimated, long-term average of BWT.

the primary cause of the curvature of the geothermal profile of Site 1006, no physical mechanism can be offered at this point to explain the difference in BWT histories between the drill sites. This is similar to the results from Leg 150, where Site 903 showed a clear concave-upward temperature profile, while Site 902, a short distance away, did not show such curvature (Mountain, Miller, Blum, et al., 1994).

Heat-Flow Variation along the Transect

As shown in Figure 8, the heat-flow values determined for Sites 1003 through 1007 seem to vary systematically with topography. Heat flow decreases inward of the Great Bahama Bank. The question here is whether this variation is associated with the seafloor topography or whether it reflects regional geothermal regime. Theoretical models on heat conduction show that topographic variation alone can affect subsurface temperature distribution (e.g., Birch, 1950; Blackwell et al., 1980). For example, if the surface temperature is uniform, a topographic depression causes a positive heat-flow anomaly, and vice versa. In the western margin of the Great Bahama Bank, seafloor elevation varies by ~660 m in a relatively short distance of 15 km. Temperature at the seafloor also varies with topography. We now attempt to quantify this effect.

In examining the topographic thermal effect, we use a simple method proposed by Blackwell et al. (1980). This method calculates the subsurface temperature distribution for a given set of surface temperature-surface elevation data, by applying a Fourier series fit in a fashion similar to the upward continuation problems in gravity and magnetics (Henderson and Cordell, 1971). It is possible to model the topographic effect in three dimensions; however, we believe a two-dimensional model along the east-west line should be adequate because this part of the Bahama platform edge is straight in the north-south direction and there is little bathymetric variation in the same direction. Sites 1003 through 1007 are located along a straight line in the southwest-northeast direction, whereas the shelf edge of the bank runs roughly north-south. Thus, in the two-dimensional model, we measure the distance between drill sites in the east-west direction, rather than along the transect line. The bathymetry of this area was previously surveyed in detail (Eberli, Swart, Malone, et al., 1997). We estimate the temperatures at the seafloor using the hydrographic data previously obtained in this part of the Straits of Florida (Leaman et al., 1995).

The modeling method of Blackwell et al. (1980) assumes that the geothermal field is in steady state. We have evaluated transient thermal effects such as sedimentation and BWT fluctuation separately from the topographic effect. We have also quantified the thermal effect of sedimentation (Table 2), and thus can estimate the heat flow without this effect. In addition, we have determined the background conductive heat flow at each site using only the temperature measurements in deep sediments free from the potential fluid flow and the BWT fluctuations. The model also assumes that subsurface thermal conductivity is uniform. The second assumption may cause errors because, in reality, thermal conductivity increases with depth because of compaction as we have discussed in modeling the thermal effect of sedimentation. More elaborate numerical methods may be used to account for this effect, if the thermal conductivity structure of the platform is better constrained. Direct conductivity measurements are available only from the five drill sites that extend to 400–1300 mbsf.

Figure 8 compares the heat-flow values at each drill site and the heat-flow variation predicted by the model. It assumes a uniform background heat flow of 43 mW/m² and a thermal conductivity of 1.25 W/(m·K). We also examined the model for thermal conductivity values of 1.0 W/(m·K) and 1.5 W/(m·K) and obtained almost identical results for the same background heat-flow value. The general shape of the model-predicted heat-flow variation matches that of the observed. It shows a peak near the foot of the bank and heat-flow decreases up slope. Thus, the topographic thermal effect can account for the general trend of heat-flow variation and its magnitude. However, on the bank slope, the observed heat-flow values are 5–10 mW/m² less than predicted. There are two possible explanations. The first is that the geometry, the assumed seafloor temperatures, and/or the thermal conductivity structure of the model contain errors. Adjusting these parameters would eventually reproduce the observed heat-flow variation without changing the background heat flow. The second is that the background heat flow of the study area varies laterally. In other words, the topographic effect alone cannot explain the observed

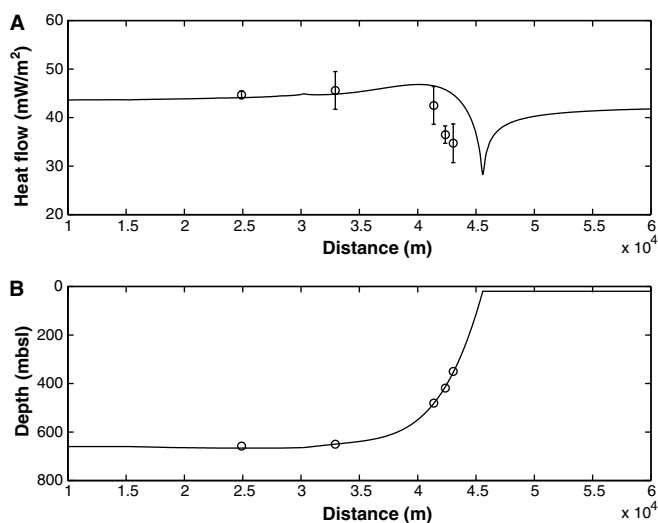


Figure 8. **A.** Comparison of the heat-flow values predicted by the thermal model that accounts for the topographic effect (solid line) and the heat-flow values determined at Sites 1003 through 1007 (open circles). **B.** The topographic profile used in the model (solid line) and the seafloor depths of the same drill sites (open circles).

heat-flow variation even if all other model parameters could be more tightly constrained.

Provided with data from only five locations along one transect of 20 km, it is difficult to further discuss this matter. We are inclined to accept the first explanation because of the similarity of the shape of the model-predicted and the observed heat-flow variation along the transect. In addition, the background heat flow of 43 mW/m² away from the bank is close to those reported in the abyssal plain of the Gulf of Mexico (41–45 mW/m²; Nagihara et al., 1996), which is the basin in the opposite side of the Florida platform. The values are reasonable for old continental margins of Jurassic age. The magnitude of the decrease in heat flow (10–15 mW/m² drop within a short distance of ~15 km) may be difficult to explain by any tectonic mechanisms associated with the ocean continent transition and/or the difference in the amount of initial continental extension. However, there is no other strong evidence for rejecting spatially variable heat flow.

CONCLUSIONS

The geothermal measurements made during and after Leg 166 have provided, for the first time, quantitative constraints to the thermal regime of the western margin of the Great Bahama Bank. Conductive heat flow through the seafloor varies systematically along the drilling transect of Sites 1003 through 1007. We believe that much of this variation is caused by topographic variation. The regional background heat flow seems nearly uniform at ~43 mW/m², a reasonable value for the tectonic setting of an old continental margin. However, we do not have any strong evidence for rejecting the possibility that background heat flow indeed decreases upslope of the bank. More reliable heat-flow data, especially from the top of the bank, are needed for further examination.

Another important finding of this study is that the thermal regime of the top 50–100 mbsf of the sediments of this area is anomalous as indicated by the curvatures of the geothermal profiles. We examined three mechanisms as the potential cause of this anomaly: (1) thermal effect of sedimentation, (2) influx of seawater into the rock formation, and (3) temporal fluctuation of BWT. We ruled out the first as the primary cause. The second mechanism may explain the thermal data from Sites 1004 and 1005 but not those from other sites, particularly Site 1006, because of the thickness discrepancy in the zones of

chemical and thermal anomalies. It is more likely that the third mechanism affected Site 1006 and possibly Sites 1003 and 1007. The history of BWT fluctuation reconstructed from the Site 1006 temperature data is very similar to the surface temperature records obtained at Key West and other parts of the east coast of the North America. However, it would probably not be consistent with the BWT histories for other drill sites of Leg 166. Perhaps, making measurements from additional closely spaced boreholes in this area would further our understanding.

ACKNOWLEDGMENTS

Trevor Lewis at Pacific Geoscience Centre made his laboratory available for the thermal conductivity measurements of the lithified core samples. Discussion with Andy Fisher at University of California, Santa Cruz, Peter Swart at University of Miami, and Earl Davis at Pacific Geoscience Centre was helpful in developing this manuscript. Kathy Schwehr at University of Houston assisted Nagihara in compiling the NOAA hydrographic data from the Straits of Florida. Funding for this work was made available by a grant from JOI U.S. Scientific Support Program.

REFERENCES

- Beltrami, H., and Mareschal, J.-C., 1991. Recent temperature changes in eastern Canada inferred from geothermal measurements. *Geophys. Res. Lett.*, 18:605–608.
- Birch, F., 1950. Flow of heat in the front range, Colorado. *Geol. Soc. Am. Bull.*, 61:567–630.
- Blackwell, D.D., Steele, J.L., and Brott, C.A., 1980. The terrain effect on terrestrial heat flow. *J. Geophys. Res.*, 85:4757–4772.
- Bredehoeft, J.D., and Papadopoulos, I.S., 1965. Rates of vertical groundwater movement estimated from the earth's thermal profile. *Water Resour. Res.*, 1:325–328.
- Budiansky, B., 1970. Thermal and thermoelastic properties of isotropic composites. *J. Compos. Mater.*, 4:286–295.
- Buffler, R.T., Schlager, W., Bowdler, J.L., et al., 1984. Site 535, 539, and 540. In Buffler, R.T., Schlager, W., et al., *Init. Repts. DSDP, 77*: Washington (U.S. Govt. Printing Office), 25–218.
- Bullard, E.C., 1939. Heat flow in South Africa. *Proc. R. Soc. London A*, 173:474–502.
- , 1954. The flow of heat through the floor of the Atlantic Ocean. *Proc. R. Soc. London A*, 222:408–429.
- Carslaw, H.S., and Jaeger, J.C., 1959. *Conduction of Heat in Solids* (2nd ed.): Oxford (Clarendon Press).
- Deming, D., 1995. Climatic warming in North America: analysis of borehole temperatures. *Science*, 268:1576–1577.
- Eberli, G.P., Kendall, C.G., Moore, P., Whittle, G.L., and Cannon, R., 1994. Testing a seismic interpretation of Great Bahama Bank with a computer simulation. *AAPG Bull.*, 78:981–1004.
- Eberli, G.P., Swart, P.K., Malone, M.J., et al., 1997. *Proc. ODP, Init. Repts.*, 166: College Station, TX (Ocean Drilling Program).
- Fisher, A.T., and Becker, K., 1993. A guide to ODP tools for downhole measurements. *ODP Tech. Note*, 7.
- Hanson, K., and Maul, G.A., 1993. Analysis of temperature, precipitation, and sea-level variability with concentration on Key West, Florida, for evidence of trace-gas-induced climatic change. In Maul, G.A. (Ed.), *Climatic Change in the Intra-Americas Seas*: London (United Nations Environmental Program), 193–213.
- Henderson, R.G., and Cordell, L., 1971. Reduction of unevenly spaced potential field data to a horizontal plane by means of finite harmonic series. *Geophysics*, 36:856–866.
- Horai, K., and Von Herzen, R.P., 1985. Measurement of heat flow on Leg 86 of the Deep Sea Drilling Project. In Heath, G.R., Burckle, L.H., et al., *Init. Repts. DSDP, 86*: Washington (U.S. Govt. Printing Office), 759–777.
- Hutchison, I., 1985. The effect of sedimentation and compaction on oceanic heat flow. *Geophys. J. R. Astron. Soc.*, 82:439–459.
- Jaeger, J.C., 1965. Application of the theory of heat conduction to geothermal measurements. In Smith, W.E. (Ed.), *Terrestrial Heat Flow*. Am. Geophys. Union, Geophys. Monogr., 8:7–21.
- Jemsek, J., Von Herzen, R.P., and Andrew, P., 1985. In-situ measurement of thermal conductivity using the continuous-heating line source method and WHOI outrigger probe. *Woods Hole Oceanogr. Inst. Tech. Rep.*, WHOI-85–28.
- Kohl, T., 1998. Paleoclimatic temperature signals: can they be washed out? *Tectonophysics*, 15:225–234.
- Lachenbruch, A., and Marshall, B.V., 1986. Changing climate: geothermal evidence from permafrost in the Alaskan Arctic. *Science*, 234:689–696.
- Leaman, K.D., Vertes, P.S., Atkinson, L.P., Lee, T.N., Hamilton, P., and Waddell, E., 1995. Transport, potential velocity, and current/temperature structure across Northwest Providence and Santaren Channels, and the Florida Current off Cay Sal Bank. *J. Geophys. Res.*, 100:8561–8569.
- Levitus, S., 1989. Interpentadal variability of temperature and salinity at intermediate depths of the North Atlantic Ocean, 1970–1974 versus 1955–1959. *J. Geophys. Res.*, 94:6091–6131.
- Levitus, S., and Antonov, J., 1995. Observational evidence of interannual to decadal-scale variability of the subsurface temperature-salinity structure of the world ocean. *Clim. Change*, 31:495–514.
- Lewis, T.J., 1975. A geothermal study at Lake Dufault, Quebec [Ph.D. dissert.]. Univ. of Ontario.
- Lister, C.R.B., Sclater, J.G., Davis, E.E., Villinger, H., and Nagihara, S., 1990. Heat flow maintained in ocean basins of great age: investigations in the north-equatorial West Pacific. *Geophys. J. Int.*, 102:603–630.
- Mountain, G.S., Miller, K.G., Blum, P., et al., 1994. *Proc. ODP, Init. Repts.*, 150: College Station, TX (Ocean Drilling Program).
- Nagihara, S., Sclater, J.G., Phillips, J.D., Behrens, E.W., Lawver, L.A., Nakamura, Y., Maxwell, A.E., Lewis, T., and Garcia-Abdeslem, J., 1996. Heat flow in the western abyssal plain of the Gulf of Mexico: implications for thermal evolution of the old oceanic lithosphere. *J. Geophys. Res.*, 101:2895–2913.
- Niiler, P.P., and Richardson, W., 1973. Seasonal variability of the Florida current. *J. Mar. Res.*, 31:144–167.
- NOAA, 1994. *World Ocean Atlas 1994, Disc 8: Standard Level Profile Data for the Atlantic and Indian Oceans*. CD-ROM NODC-50.
- Parrilla, G., Lavin, A., Bryden, H., Garcia, M., and Millard, R., 1994. Rising temperatures in the subtropical North Atlantic Ocean over the past 35 years. *Nature*, 369:48–51.
- Parsons, B., and Sclater, J.G., 1977. An analysis of the variation of ocean floor bathymetry and heat flow with age. *J. Geophys. Res.*, 82:803–827.
- Pollack, H.N., and Chapman, D.S., 1993. Underground records of changing climate. *Sci. Am.*, 268:44–50.
- Roemmich, D., and Wunsch, C., 1984. Apparent changes in the climatic state of the deep North Atlantic Ocean. *Nature*, 307:447–450.
- Schlager, W., Buffler, R.T., Angstadt, D., and Phair, R., 1984. Geologic history of the southwestern Gulf of Mexico. In Buffler, R.T., Schlager, W., *Init. Repts. DSDP, 77*: Washington (U.S. Govt. Printing Office), 715–738.
- Sclater, J.G., and Christie, P.A.F., 1980. Continental stretching: an explanation of the post-mid-Cretaceous subsidence of the central North Sea basin. *J. Geophys. Res.*, 85:3711–3739.
- Shen, P.Y., and Beck, A.E., 1991. Least squares inversion of borehole temperature measurements in functional space. *J. Geophys. Res.*, 96:19965–19979.
- Shen, P.Y., Pollack, H.N., Huang, S., and Wang, K., 1995. Effects of subsurface heterogeneity on the inference of climate change from borehole temperature data: model studies and field examples from Canada. *J. Geophys. Res.*, 100:6383–6396.
- Turcotte, D.L., and Schubert, G., 1982. *Geodynamics: Applications of Continuum Physics to Geological Problems*: New York (Wiley).
- Von Herzen, R.P., and Maxwell, A.E., 1959. The measurement of thermal conductivity of deep-sea sediments by a needle-probe method. *J. Geophys. Res.*, 64:1557–1563.
- Von Herzen, R.P., and Uyeda, S., 1963. Heat flow through the Pacific Ocean floor. *J. Geophys. Res.*, 68:4219–4250.
- Wang, K., 1992. Estimation of ground surface temperatures from borehole temperature data. *J. Geophys. Res.*, 97:2095–2106.
- Wang, K., and Davis, E.E., 1992. Thermal effects of marine sedimentation in hydrothermally active areas. *Geophys. J. Int.*, 110:70–78.
- Wang, K., and Lewis, T.J., 1992. Geothermal evidence from Canada for a cold period before recent climatic warming. *Science*, 256:1003–1005.
- Wang, K., Lewis, T.J., and Jessop, A.M., 1992. Climatic changes in central and eastern Canada inferred from deep borehole temperature data. *Palaeogeogr., Palaeoclimatol., Palaeoecol.*, 98:129–141.

Date of initial receipt: 31 July 1998

Date of acceptance: 26 July 1999

Ms 166SR-123